University of South Bohemia
Faculty of Science

Functional characterization of the insulin signaling pathway in the hard tick *Ixodes ricinus*

RNDr. thesis

Mgr. Tereza Kozelková

České Budějovice 2024

RNDr. thesis:

Kozelková, T., 2024: Functional characterization of the insulin signaling pathway in the hard tick *Ixodes ricinus*. RNDr. Thesis, in English – 10 p., Faculty of Science, University of South Bohemia, České Budějovice, Czech Republic.

Annotation

In this thesis, the molecular and functional characterization of the insulin receptor signaling pathway (ISP) in hard tick *Ixodes ricinus* was characterized. As obligatory blood-feeding ectoparasites, ticks play a crucial role in the transmission of various pathogens, including bacteria, viruses, and protozoa, which has a significant impact on human and animal health. The parasite is strictly bonded with its host through a unidirectional transmission of nutrition for its survival, development, and reproduction. The ISP, a highly conserved system, regulates numerous physiological and anabolic processes to nutritional availability. This study aims to investigate the functionality of key components of the ISP pathway identified in the midgut transcriptome, namely the insulin receptor (*Ir*InR), the protein kinase B called AKT (*Ir*AKT), and the target of rapamycin (*Ir*TOR). To achieve this goal, the expression profiles of these components in tick tissues during feeding and after detachment were investigated using qRT-PCR. Additionally, RNAi silencing of individual components was performed, and the phenotype of the ticks was observed. To further clarify the effects of ISP, immunization of rabbits with recombinant *Ir*InR protein and tick infestation were investigated.

Declaration:

I declare that I am the author of this qualification thesis and that I have used only the sources and literature indicated in the list of sources for the preparation of this thesis.

České Budějovice 22.1. 2024

.....

This thesis is based on following publication:

Kozelková, T., Doležel, D., Grunclová, L., Kučera, M., Perner, J., & Kopáček, P. (2021). Functional characterization of the insulin signaling pathway in the hard tick Ixodes ricinus. *Ticks and tick-borne diseases*, *12*(4), 101694. https://doi.org/10.1016/j.ttbdis.2021.101694

I declare that I participated significantly in the publication by investigation, data curation, and writing – original draft.

My total share in this publication was 60 %.

Ticks and Tick-borne Diseases 12 (2021) 101694

Contents lists available at ScienceDirect

Ticks and Tick-borne Diseases

journal homepage: www.elsevier.com/locate/ttbdis

Functional characterization of the insulin signaling pathway in the hard tick *Ixodes ricinus*

Tereza Kozelková [a,b], David Doležel [c], Lenka Grunclová [a], Matěj Kučera [a,b], Jan Perner [a], Petr Kopáček [a,*]

[a] Institute of Parasitology, Biology Centre of the Czech Academy of Sciences, Branišovská 31, 370 05, České Budějovice, Czech Republic
[b] Faculty of Science, University of South Bohemia, Branišovská 31, 370 05, České Budějovice, Czech Republic
[c] Institute of Entomology, Biology Centre of the Czech Academy of Sciences, Branišovská 31, 370 05, České Budějovice, Czech Republic

ARTICLE INFO

Keywords:
Tick
Ixodes ricinus
Insulin receptor
AKT
TOR
RNA interference

ABSTRACT

Ticks are blood-feeding arachnids transmitting a variety of pathogens to humans and animals. A unique trait in tick physiology is their ability to engorge and digest large amounts of host blood, ensuring their high reproductive potential. Activation of the blood digestive machinery in the tick gut, as well as processes controlling maturation of ovaries, are triggered upon blood meal uptake by still largely unknown mechanisms. Sensing of the nutritional status in metazoan organisms is facilitated by the evolutionarily conserved Insulin Signaling Pathway (ISP) and the interlinked Target of Rapamycin (TOR) pathway. Recently, we have identified three components of these pathways in the hard tick *Ixodes ricinus* midgut transcriptome, namely a putative insulin receptor (InR), and the downstream intracellular serine/threonine kinases AKT and TOR.

In this study, we primarily focus on the molecular and functional characterization of the *I. ricinus* insulin receptor (*Ir*InR), the first InR characterized in Chelicerates. A phylogenetic analysis across the major Arthropod lineages demonstrated that ticks possess only one gene encoding an InR-related molecule. Tissue expression profiling by quantitative PCR in semi-engorged *I. ricinus* females revealed that the *Ir*InR, as well as AKT (*Ir*AKT) and TOR (*Ir*TOR) are expressed in various organs, with the highest expression being detected in ovaries.

We have further evaluated the impact of RNAi-mediated knock-down (KD) of *Ir*InR, *Ir*AKT, and *Ir*TOR on tick blood-feeding and reproductive capacity. Weights of engorged *Ir*InR KD females and laid egg clutches were reduced compared to the control group, and these quantitative parameters clearly correlated with the efficiency of RNAi-KD achieved in individual ticks. The most striking phenotype was observed for *Ir*AKT KD that impaired tick feeding and completely aborted egg production. A recombinant extracellular fragment of the *Ir*InR α-subunit was used to produce antibodies in experimental rabbits to assess its potential as a protective antigen against tick feeding and reproduction.

Our data clearly indicate the functionality of the ISP in ticks and demonstrate the need for further investigation of specific roles played by the endogenous insulin-like peptides in tick physiological processes.

1. Introduction

Ticks are globally important parasites and vectors of a wide variety of agents infectious to humans, livestock or wildlife (de la Fuente et al., 2008). During hundreds of millions of years of evolution of an ancestral mite to an obligatory blood-feeding lifestyle, ticks have acquired a number of specific physiological traits that separate these ectoparasites from other arthropod blood-feeders as well as their vertebrate hosts (Mans et al., 2016). A fascinating trait in tick physiology, not common to any other hematophagous parasite, is their capability to ingest extreme amounts of blood (Kaufman, 2007). An adult hard tick female, such as the European Lyme borreliosis spirochete vector *Ixodes ricinus*, engorges amounts of ingested host blood that exceeds by more than one hundred times the weight of the unfed tick, and converts the acquired nutrients into the production of thousands of laid eggs (Sonenshine and Roe, 2014). However, despite its importance, the knowledge of mechanisms controlling blood meal digestion and subsequent processes involved in tick development and reproduction are still very limited.

* Corresponding author.
E-mail address: kopajz@paru.cas.cz (P. Kopáček).

https://doi.org/10.1016/j.ttbdis.2021.101694
Received 3 November 2020; Received in revised form 21 January 2021; Accepted 15 February 2021
Available online 25 February 2021

In metazoan organisms, the insulin signaling pathway (ISP), together with the downstream inter-linked target of rapamycin (TOR) pathway are evolutionarily conserved mechanisms acting as sensors of nutritional status and control a variety of metabolic and physiological processes including reproduction (Badisco et al., 2013). The first component of ISP is the transmembrane insulin receptor (InR) that becomes activated upon binding of its agonist insulin or, more generally, insulin-like peptides (ILPs) (De Meyts and Whittaker, 2002). Vertebrates possess three different InRs that could bind insulin or insulin-like growth factors, while the presence of only one gene encoding InR-related molecules had previously been identified in invertebrates (Hernandez-Sanchez et al., 2008). However, multiple InRs have been found in several insect orders, and phylogenetic reconstruction points to major duplications (and losses) of InR in insects (Kremer et al., 2018; Smykal et al., 2020). Since the discovery of the first ILP termed bombyxin from the silk moth (Nagasawa et al., 1984), the ISP and its components have been widely explored in insect physiology and innate immunity (Ahlers et al., 2019; Luckhart and Riehle, 2007; Vafopoulou, 2014).

By contrast, the knowledge of ISP in ticks and other arachnids is still rather limited and lags far behind insects. The first reports about the possible presence of ILPs in synganglions (brain-like organs) of two tick species were based on positive immunoreactions with anti-human insulin antibodies (Davis et al., 1994; Zhu and Oliver, 1991). The existence of insulin-responsive machinery was later demonstrated in *in vitro* studies using the BME26 cell line derived from embryonic cells of the cattle tick *Rhipicephalus* (formerly *Boophilus*) *microplus,* where the addition of exogenous (human) insulin into the culture resulted in elevated levels of cell glycogen (de Abreu et al., 2009). A transcript encoding tick ILP has been identified in the synganglion transcriptome from the American dog tick *Dermacentor variabilis* (Donohue et al., 2010). More recently, four genes encoding ILPs from the genome of the blacklegged tick, *Ixodes scapularis* have been identified and characterized (Sharma et al., 2019a). The physiological function of serine/threonine kinases TOR and AKT have been examined by RNA interference in the hard tick *Haemaphysalis longicornis* (Umemiya-Shirafuji et al., 2012a, b). These studies demonstrated that *Hl*TOR plays an important role in vitellogenesis and production of eggs (Umemiya--Shirafuji et al., 2012a) while *Hl*AKT is essential for completing the processes associated with blood-feeding (Umemiya-Shirafuji et al., 2012b). Another study of the role of three components of the ISP and TOR signaling pathways (AKT, TOR and glycogen synthase kinase - GSK3) in embryogenesis of *R. microplus* was reported recently (Waltero et al., 2019).

In our previous midgut transcriptome study of *I. ricinus*, we identified a number of transcripts encoding molecules potentially involved in nutritional uptake, sensing and signaling (Perner et al., 2016a). Among them, three putative components of *I. ricinus* ISP were found to be expressed in the tick midgut, namely the InR (*Ir*InR, Ir-120837), AKT (*Ir*AKT, Ir-103659), and TOR (*Ir*TOR, IrSigP-108190).

In this work, we mainly focus on the molecular and functional characterization of *Ir*InR, as this receptor has not yet been (to the best of our knowledge) functionally characterized in any chelicerate, including ticks. In addition, we also examined the phenotypes of *I. ricinus* TOR (*Ir*TOR) and AKT (*Ir*AKT) upon their RNAi-mediated knock down (KD) to evaluate the potential of these intracellular kinases as drug targets.

2. Materials and methods

2.1. Ticks and animals

Adult females and males of *I. ricinus* were collected by flagging around Ceske Budejovice, the Czech Republic, and maintained in separate vials in the animal rearing facility of the Institute of Parasitology, with a humidity of about 95 %, temperature of 24 °C, and day/night period set to 15/9 h. For most experiments described below, *I. ricinus* females were fed naturally on laboratory guinea pigs, while laboratory rabbits were used for vaccination experiments. All laboratory animals were treated in accordance with the Animal Protection Law of the Czech Republic No. 246/1992 Sb., ethics approval No. 25/2018.

2.2. Identification of genes and phylogenetic analysis

Transcripts encoding *Ir*InR were identified in transcriptomes from partially or fully fed *I. ricinus* females, namely transcript Ir-120837 from the midgut (Perner et al., 2016a), and Ir-SigP-26449_FR1_99-1649 from salivary glands (Perner et al., 2018). Their similarity to insulin receptor or insulin-like growth factor receptor transcripts of other organisms were confirmed by BLAST analyses (National Center for Biotechnology Information (NCBI), National Institute of Health; https://blast.ncbi.nlm.nih.gov/Blast.cgi). For alignment of the sequences, ClustalOmega (https://www.ebi.ac.uk/Tools/msa/clustalo/) using the ClustalW method was used and presented using BoxShade (https://embnet.vital-it.ch/software/BOX_form.html) software. The signal peptide was predicted using the SinalP server (http://www.cbs.dtu.dk/services/SignalP/). Protein domains were identified on-line with InterPro (https://www.ebi.ac.uk/interpro/search/sequence/). InR from vertebrates, molluscs, insects and crustaceans were retrieved from GenBank (https://www.ncbi.nlm.nih.gov/genbank/). Remaining chelicerate InRs were identified in the GenBank protein database and transcriptome shotgun assemblies (TSAs) using BLASTP and tBLASTn, respectively. Protein sequences were aligned using the ClustalW algorithm in Geneious Prime (www.geneious.com), poorly aligned variable N- and C- termini were manually trimmed, and the resulting alignment is available on request. The phylogenetic tree was reconstructed using W-IQ-TREE 1.6.11 (http://iqtree.cibiv.univie.ac.at; (Trifinopoulos et al., 2016)) under the WAG + F+I + G4 model (identified as the Best-fit model) with 100 bootstrap replicates (standard). The tree was visualized in FigTree v1.4.4 (http://tree.bio.ed.ac.uk/software/figtree/) and the taxonomic description was added in Adobe Illustrator.

2.3. Total RNA isolation and relative expression profiling by qRT-PCR

Tissues (ovaries, salivary glands, tracheae with fat body, midgut, Malpighian tubules and the rest of the body) were dissected from semi-engorged *I. ricinus* females (fed for 5 d) under a drop of DEPC (diethylpyrocarbonate) PBS (8 % NaCl, 0.2 % KCl, 1.8 % Na_2HPO_4, 0.14 % KH_2PO_4 in 1 000 mL of 0.1 % DEPC-treated distilled H_2O, pH = 7, autoclaved). For the determination of expression dynamics during feeding and after detachment, ovaries were dissected from *I. ricinus* females after the following time intervals: unfed, fed for 1, 3, 5 d, fully fed, and ticks 3, 6 and 12 d after detachment from the guinea pig. Total RNA was extracted from tissues using Nucleo-SpinRNA II Kit (Macherey-Nagel, Düren, Germany), the samples were treated with the recombinant DNase (CAS 9003-98-9) on a silica membrane according to the manufacturer's protocol and the absence of genomic DNA traces was verified by the agarose gel electrophoresis. The concentration of eluted total RNA was determined using a Nanodrop UV–vis spectrophotometer (Thermo Fisher Scientific; Waltham, MA, USA) and 200 ng of the RNA isolate was transcribed into cDNA using the Transcriptor High-Fidelity cDNA Synthesis Kit (Roche Diagnostics GmbH; Mannheim, Germany) and oligo-dT primers according to the manufacturer's manual. Samples were analyzed in independent technical and biological triplicates by the quantitative real-time PCR (qRT-PCR) using a LightCycler 480 (Roche Diagnostics GmbH); and Fast Star Universal SYBR Green Master Mix (Roche Diagnostics GmbH) and primer pairs *InR F – InR R*, *AKT F – AKT R*, and *TOR F – TOR R* (Supplementary Table S1) for amplification of *Ir*InR, *Ir*AKT, and *IrTOR,* respectively. The amplification program consisted of initial denaturation at 95 °C for 5 min, followed by 50 cycles of denaturation at 95 °C for 20 s, annealing at 60 °C for 30 s and extension at 72 °C for 30 s. The relative expression was calculated using the mathematical model of the ΔΔCt method (Pfaffl, 2001) and normalized to elongation factor-1α (*ef1α*) (Nijhof et al., 2009) using *EF F* and *EF R*

primers (Supplementary Table S1).

2.4. RNA interference

Fragments of *Ir*InR, *Ir*AKT, and *Ir*TOR genes were PCR amplified using cDNA from ovaries of semi-engorged *I. ricinus* females as a template. Primer pairs *InR-apa – InR-xba*, *AKT-apa – AKT-xba*, and *TOR-apa – TOR-xba* (Supplementary Table S1), were designed based on the respective sequences using Primer Blast (https://www.ncbi.nlm.nih.gov/tools/primerblast/), Primer 3 Input (http://primer3.ut.ee/), and Restriction Mapper (http://www.restrictionmapper.org/). The amplicons were purified from a 2% agarose gel using Gel and PCR Clean-up Kit (Macherey-Nagel). *Ir*InR, *Ir*AKT, *Ir*TOR, and the control green fluorescent protein (GFP) dsRNAs were synthesized using the MEGAscript T7 transcription kit (Ambion; Vilnius, Lithuania) according to the previously described protocol (Hajdusek et al., 2009). Unfed *I. ricinus* females were injected with 0.5 µl (3 µg/µl) of respective dsRNAs, or GFP dsRNA in the control group and maintained at 24 °C to rest for one day. The females were then allowed to feed naturally on guinea pigs in the presence of an equal number of males until replete, except for three ticks from each group that were forcibly removed on the 3rd day of feeding to examine the level of RNAi KD in ovaries by qRT-PCR. The engorged ticks were visually checked, weighed, and maintained in separate vials to evaluate oviposition by weighing egg clutches and visual scoring of the hatching success: (0) - none; (+) ~30 %; (++) ~50−60%; (+++) ~80−100% hatching rate.

2.5. Experimental vaccination of rabbits with recombinant IrInR fragment for protection against tick infestation

The gene product of 906 bps encoding the 33 kDa fragment of the *Ir*InR N-terminal extracellular portion was PCR amplified using cDNA from ovaries of semi-engorged *I. ricinus* females as a template and primers *InR_pET100S2* and *InR_pET100AS2* primers (Supplementary Table S1). The PCR product was cloned into the pET100/D-TOPO vector of Champion™ pET directional expression kit (Invitrogen, Carlsbad, CA, USA) expressed in *E. coli* BL21 Star™ (DE3) competent cells, purified and refolded as described previously (Hajdusek et al., 2010). The recombinant *Ir*InR fragment (100 µg/mL) was mixed with incomplete Freund́ s adjuvant (Sigma-Aldrich; St. Louis, MO, USA (1:1) and used to immunize three rabbits in four doses (weeks 1, 3, 5 and 7). One negative control rabbit was injected with incomplete Freund́ s adjuvant only. Two weeks after the last immunization, blood samples were collected from the rabbits' ears to examine the specific reaction of immune sera with the recombinant *Ir*InR antigen by Western blot analysis. Rabbits were then infested with 50 unfed *I. ricinus* females placed in two cylinders glued on the shaven backs of immunized rabbits (in the presence of an equal number of males) and allowed to feed naturally until replete. Engorged ticks were visually checked, weighed, and maintained in separate vials as described above to evaluate oviposition by weighing egg clutches and by scoring larval hatching (see above).

2.6. Statistics

Statistical analysis was performed in GraphPad Prism version 6.04 for Windows (GraphPad Software; San Diego, CA, USA; www.graphpad.com). Data were analyzed by ANOVA or non-parametric Mann-Whitney test. Mean (±SD, standard deviation) or median (IQR, interquartile rates) values were counted from the biological triplicates (independent experiments) and used for the graphical representations of the results and their statistical analyses (for details, see the figure legends). A P-value of <0.05 was considered as statistically significant.

3. Results

3.1. Sequence and phylogenetic analysis of the I. ricinus insulin receptor

The sequence encoding *Ir*InR (deposited in GenBank under accession No. MN207065) was completed from transcript Ir-120837 (GenBank GEFM01005395) identified in the *I. ricinus* midgut transcriptome (Perner et al., 2016a) and transcript Ir-SigP-26449_FR1_99-1969 (GenBank GEGO01006582) obtained from RNAseq analysis of *I. ricinus* salivary glands (Perner et al., 2018). The 4581 bp long cDNA encodes the *Ir*InR precursor (GenBank QGN03467) of 1526 amino-acid residues with a theoretical mass of 168.3 kDa, including a 21 amino acid-long signal peptide and both α and β subunits of 80.6 kDa and 65 kDa, respectively, presumably post-translationally cleaved in the conserved arginine-rich motif (Supplementary Fig. S1). Multiple sequence alignments with insulin receptors from selected vertebrates and invertebrates (Supplementary Fig. S1), as well as *in-silico* prediction of conserved domains (Fig. 1A), confirmed the correct identification of *Ir*InR as the insulin receptor. In order to exclude the possibility of gene duplication of InRs in ticks, as described in numerous metazoan organisms (Smykal et al., 2020), we performed phylogenetic analysis of arthropod InRs from 24 acari (ticks and mites), 6 arachnids (including 2 species of scorpions), horseshoe crab (*Limulus polyphemus*), representative hexapods (insects, Collembolla), and *Daphnia*. Mollusks, sea urchin and vertebrates served as outgroups. The tree topology was consistent with the evolution of particular taxonomic groups, including arthropod lineages, where *Ir*InR was unambiguously nested within Parasitiformes next to the InR of remaining tick species (Fig. 1B). In the case of the horseshoe crab, two InR paralogs were identified, whereas only one InR gene was present in all remaining chelicerates. Monophyly of *Limulus* with Aranea and Scorpiones was strongly supported (bootstrap 99 %), clearly suggesting a *Limulus*-specific gene duplication event, independent of InR multiplication observed in insects (included within Hexapoda). Furthermore, the position of InR from mollusks and deuterostomian lineages, represented by sea urchin (Strongylocentrotus), and vertebrates, also agrees with the expected phylogenetic relationship. In vertebrates, two additional gene duplications led to the InR-related receptor (IRR) and insulin-like growth factor 1 receptor (IGF1R) genes. Thus, the analysis also clearly revealed that all arthropod InRs are *bona fide* insulin receptors, despite their occasional annotation as IRR-like or IGF1R-like genes.

3.2. Sequences of I. ricinus serine/threonine kinases IrAKT and IrTOR

The transcript Ir-103659 (GenBank GEFM01002729) from the *I. ricinus* midgut transcriptome (Perner et al., 2016a) contained the full 1593 bp long nucleotide sequence encoding a protein of 530 amino-acid residues (predicted mass 60.2 kDa). The protein sequence (GenBank JAP73067) lacks the signal peptide and consists of highly conserved PH (Pleckstrin homology) and C-terminal serine/threonine kinases domains and its multiple amino-acid sequences alignment with homologous proteins from other organisms (Supplementary Fig. S2) confirmed its annotation as *Ir*AKT (deposited in the GenBank under accession No. MN207064).

The full coding sequence of *I. ricinus* target of rapamycin (*Ir*TOR) (deposited in the GenBank under accession No. MN207063) was completed from three overlapping transcripts IrSigP-108190, IrHemSgMg-240809, and Ir-238238 from *I. ricinus* midgut (Perner et al., 2016a), hemocytes (Kotsyfakis et al., 2015b), and salivary glands (Perner et al., 2018). The 7518 bp long mRNA encodes a protein of 2505 amino acids (GenBank QGN03465) with the theoretical mass of 284.2 kDa lacking a signal peptide and containing only one large phosphatidylinositol kinase domain belonging to the TEL1 superfamily. BLAST analysis as well as multiple amino-acid sequence alignment (Supplementary Fig. S3) confirmed its homology to the selected proteins annotated as TORs.

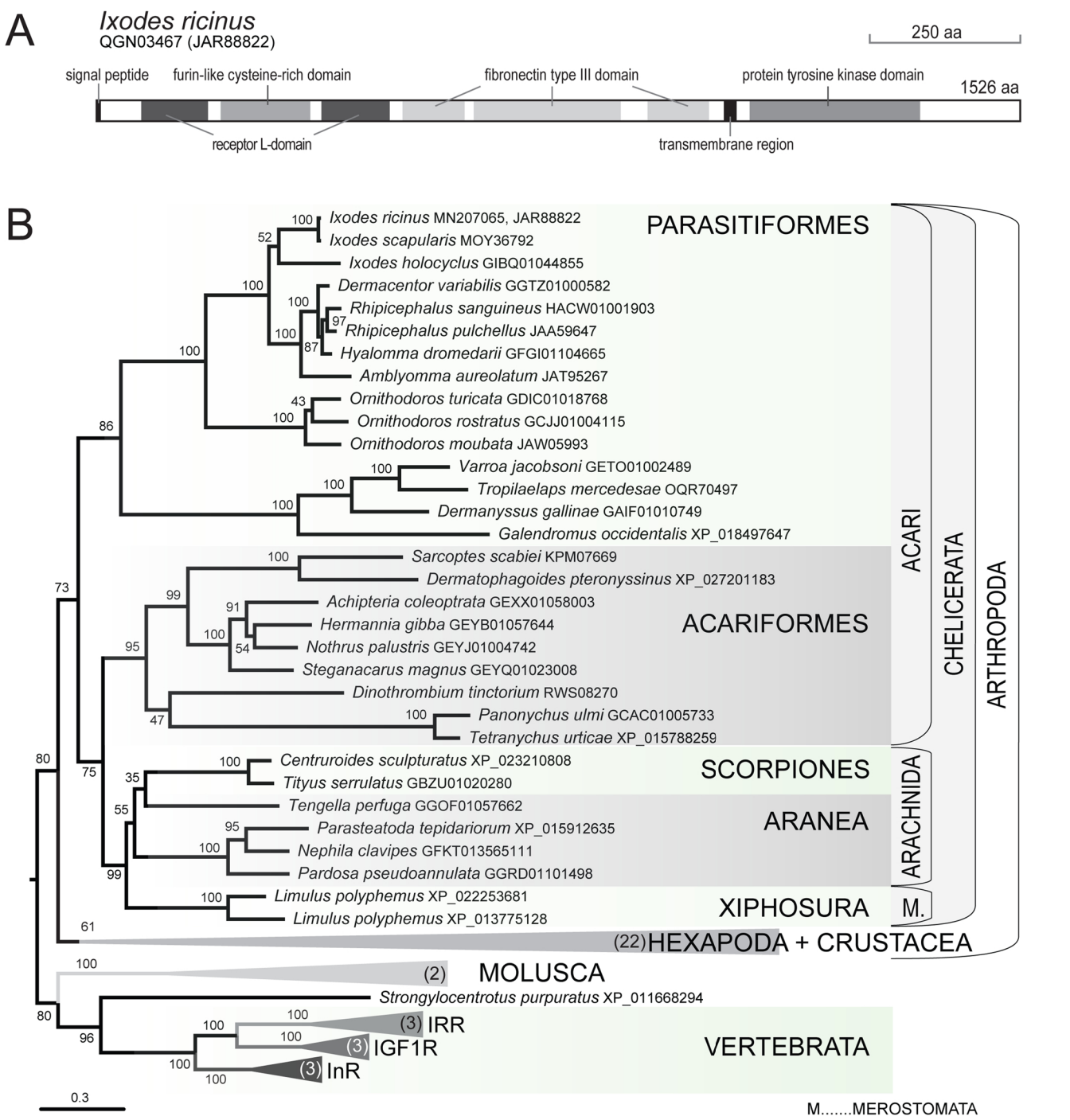

Fig. 1. *In silico* analysis of *Ixodes ricinus* insulin receptor (*Ir*InR). (A) schematic depiction of protein domains recognized in the *Ir*InR protein sequence (GenBank QGN03467) reconstructed from transcript JAR88822. (B) phylogenetic tree of arthropod insulin receptors where mollusks, sea urchin, and vertebrate sequences served as outgroups. The numbers in condensed branches indicate the numbers of species studied. The topology was inferred using W-IQ-TREE 1.6.11 maximum likelihood algorithm with WAG + F+I + G4 model (LogL = -99721.039). The branching support (>50 %) is shown as the bootstrap values calculated from 100 replicates.

3.3. *Expression profiling of IrInR, IrAKT, and IrTOR in I. ricinus tissues*

Even though the transcripts encoding *Ir*InR, *Ir*AKT, and *Ir*TOR were first identified in the *I. ricinus* midgut transcriptome (Perner et al., 2016a) we also examined the expression of the corresponding genes by qRT-PCR analysis in other tissues that can be dissected from semi-engorged *I. ricinus* females. This tissue expression profile revealed the highest levels of *Ir*InR transcript in the ovaries and to a lower extent in the midgut, salivary glands, Malpighian tubules, fat-body associated with trachea, and the rest of the body (Fig. 2A). The *Ir*InR mRNA levels in ovaries gradually increased during the course of on-host feeding, reaching their maxima in fully-fed females and then remained relatively stable over the entire off-host digestion period and vitellogenesis (Fig. 2B). A similar tissue transcription profiles with the highest expression in the ovaries and the gradual increase of mRNA levels during feeding was also observed for the downstream kinases *Ir*AKT and *Ir*TOR (Fig. 2C–F, respectively). These data implicate functioning of the ISP across tissues, indicating presence of systemic signaling pathway of tick

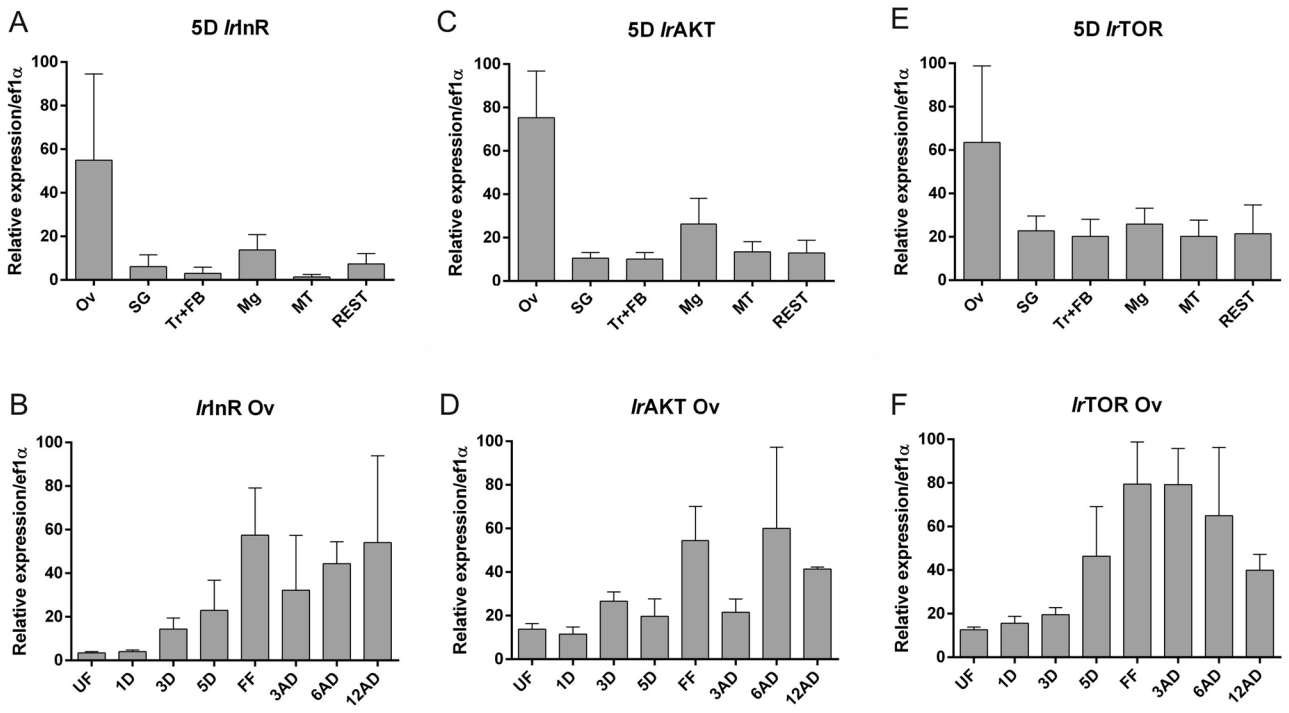

Fig. 2. *Ir*InR, *Ir*AKT, and *Ir*TOR tissue expression profiling and expression dynamics in ovaries of *Ixodes ricinus* during feeding and after detachment. Relative quantitative real-time PCR (qRT-PCR) profiling of *Ir*InR, *Ir*AKT, and *Ir*TOR in tissues of semi-engorged females (**A, C, E**) and during feeding in ovaries (**B, D, F**), respectively. Ov – ovaries, SG – salivary glands; Tr + FB – trachea + fat body; Mg – midgut; MT – Malpighian tubules; REST – rest of body; UF – unfed ticks; 1D – one day of feeding; 3D – three days of feeding; 5D – five days of feeding; FF – fully fed females; 3AD – three days after detachment; 6AD – six days after detachment; 12AD – twelve days after detachment. Each column represents the mean of biologically and technically independent triplicates; error bars indicate standard deviations.

feeding status.

3.4. *Functional assessment of I. ricinus ISP components by RNA interference*

To assess the phenotype of the *Ir*InR KD, three independent RNAi KD experiments of *Ir*InR transcripts were performed. Unfed *I. ricinus* females were injected with *Ir*InR dsRNA or GFP dsRNA for control and allowed to feed on guinea pigs until replete. To evaluate the efficiency of RNAi KD, the mRNA levels were qRT-PCR quantified in ovaries dissected from three females representing each cohort that were forcibly removed on the 3rd day of feeding. The efficiency of RNAi KD markedly differed in two out of three independent biological replicates in which gene expression was reduced to 13 %, 11 % compared to the GFP control (Fig. 3A). To assess the capacity of the ticks to fully engorge, likely through insulin-mediated nutritional status sensing, we allowed *Ir*InR KD females to feed naturally on the guinea pigs and compared their engorged weights with the control ticks injected with GFP dsRNA. The weights and body sizes of *Ir*InR dsRNA-injected engorged females were significantly lower than the control group (Fig. 3B). A statistically significant reduction was also obtained in the weights of laid eggs (Fig. 3C) however, with no apparent differences in larval hatching (data not shown). As we observed a wide range of weights of fully engorged IrInR KD ticks ranging from 170 to 420 mg (Fig. 3B), we enquired to correlate achieved engorged weight (size) with RNAi efficiency. The most obvious size differences between the GFP dsRNA-injected and *Ir*InR dsRNA-injected females were noted towards the end of feeding (7d). To demonstrate the correlation of the observed phenotype with the level of RNAi KD, we have selected five representative females from the GFP cohort and ten females from the *Ir*InR KD cohort that were further visually divided into large and small group (five each). The relative *Ir*InR expression was verified in the ovaries from each individual female by qRT-PCR. The results shown in the Fig. 3D clearly demonstrate the relationship between the tick size and the efficiency of RNAi KD.

As an alternative to RNA interference, we examined the effect of injecting the commercial insulin receptor antagonist S691 (IRA), which was previously shown to inhibit insulin action in mammalian systems *in vitro* and *in vivo* (Schaffer et al., 2008). However, the injection of 200 ng of IRA into unfed *I. ricinus* females had no statistically significant effect on tick feeding nor oviposition (Supplementary Fig. S4).

Further investigation of the roles of the downstream kinases *Ir*AKT and *Ir*TOR in tick ISP by RNAi resulted in an efficient and reproducible reduction of their mRNA levels to 3 % and 24 % (Fig. 4A, B), respectively. The most striking phenotype exerted by the *Ir*AKT KD ticks was that they were mostly not capable of completing their blood feeding during the markedly prolonged feeding times of 10–12 d (Fig. 4C). After dropping off the guinea pigs, the *Ir*AKT dsRNA injected females did not succeed in laying eggs (Fig. 4D). The weights of *Ir*TOR KD females as well as the success of oviposition (weight of laid eggs) were slightly, yet statistically significantly reduced compared to the GFP control group (Fig. 4C, D).

3.5. *Experimental vaccination of the rabbits with IrInR recombinant protein*

The promising phenotype upon *Ir*InR KD (Figs. 3), encouraged us to perform experimental vaccination of rabbits with a recombinant extracellular portion of *Ir*InR (Supplementary Fig. S1, Fig. 5A). Three rabbits were immunized with *Ir*InR recombinant protein in four doses and one control rabbit was immunized with incomplete Freund's adjuvant only. After the last immunization, blood was taken from the rabbits' ears and the production of the *Ir*InR-specific antibodies was verified by Western blot analysis (Fig. 5B). Despite the strong and specific reaction of sera from immunized rabbits with the recombinant antigen, no impairment of tick infestation or ability to produce eggs was observed (Figs. 5 C, D), which disqualifies the recombinant extracellular domain of *Ir*InR from being used as a candidate protective antigen.

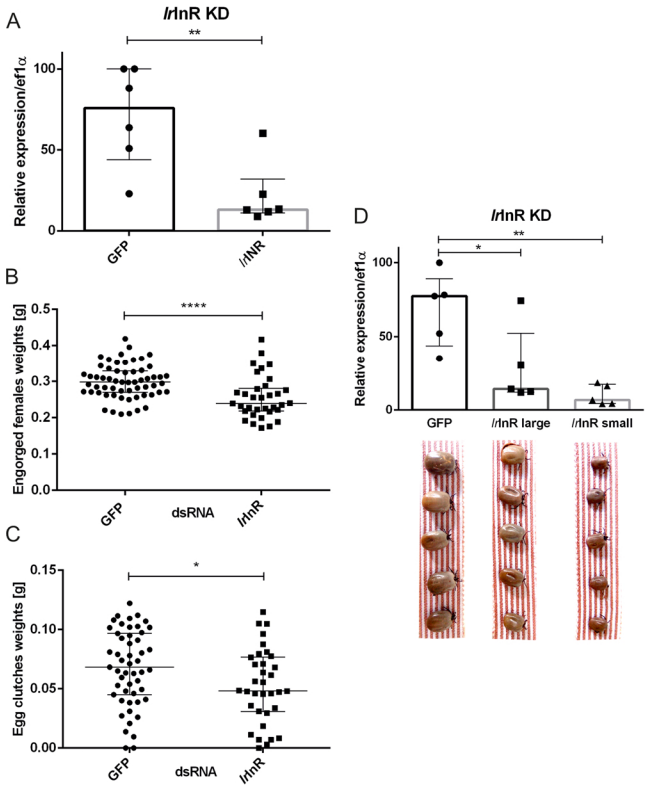

Fig. 3. RNAi knock down of *Ir*InR and the effect on *Ixodes ricinus* phenotype. (A) Verification of *Ir*InR RNAi KD efficiency from two independent experiments (three randomly selected females fed for 3 d were examined from each cohort). (**B**) The weight differences of *Ir*InR dsRNA injected females compared to the GFP control group. (**C**) The weights of eggs laid by *Ir*InR dsRNA injected females compared to the GFP control group. Data were analyzed by the Mann-Whitney test: A—P = 0.0087; B—P < 0.0001; C—P = 0.0343. (**D**) Relationship between body size and the efficiency of RNAi KD of *Ir*InR. Upper panel – Relative *Ir*InR mRNA expressions in ovaries in each group of individual ticks. Lower panel – Images of the individual control (GFP dsRNA) females and two groups (large and small) of *Ir*InR dsRNA-injected females used for the analysis. Each *Ir*InR group was compared to the GFP control group using the Mann-Whitney test P = 0.0317 (GFP vs. *Ir*InR - large) and P = 0.0079 (GFP vs. *Ir*InR - small). Lines or columns indicate the medians; error bars indicate the interquartile rates.

4. Discussion

In this work we have functionally characterized an insulin receptor, *Ir*InR, and downstream kinases *Ir*AKT and *Ir*TOR, whose transcripts were previously identified in the midgut transcriptome (Perner et al., 2016a). To the best of our knowledge, an insulin receptor has not yet been explored in any tick species and thus its functional characterization can contribute to and complement the scarce and fragmented information available about components of ISP in ticks (Sharma et al., 2019a; Umemiya-Shirafuji et al., 2012a, b; Waltero et al., 2019). The identification of *Ir*InR as an insulin receptor was unambiguously confirmed by multiple amino-acid sequence alignments with representative InRs from selected organisms (Supplementary Fig. S1) as well as by the conserved arrangement of the signature protein domains (Fig. 1A).

Given the complex evolution of insulin receptors and related variants of InR (Smykal et al., 2020), further complicated by various annotations of tick receptors in GenBank, we first performed a systematic reconstruction of InR evolution in the major Arthropod lineages, with particular focus on Chelicerates. Notably, our analysis revealed taxon-specific InR duplication in the horseshoe crab. Similar independent InR gene multiplications were previously reported in Plathelminthes, Nematoda, *Daphnia* (Crustacea), and insects (for most recent overview see (Smykal et al., 2020). In the case of insects, the InR duplication allowed versatile regulation of wing polymorphism by ISP (Lin et al., 2018; Smykal et al., 2020; Xu et al., 2015). Similarly, IRR and IGF1R originated from vertebrate-specific duplication, and, together with ligand coevolution, provide yet another level of complexity in the regulation of vertebrate metabolism and development (De Meyts and Whittaker, 2002; Dupont and LeRoith, 2001). Whether *Limulus* InRs have distinct or identical roles is, at this point, unclear.

Tissue expression profiling of *Ir*InR mRNAs revealed that this transcript is not solely gut specific but is present in other tissues, with the highest expression in ovaries (Fig. 2A, B). We observed almost identical tissue expression and dynamic expression profiles for the downstream kinases *Ir*TOR and *Ir*AKT (Fig. 2C–F), which is in agreement with the data published for TOR and AKT expression in *H. longicornis* (Umemiya-Shirafuji et al., 2012a, b). Ubiquitous expression of InR in multiple tissues was reported for the model insect *Drosophila melanogaster* (reviewed in (Wu and Brown, 2006), with the highest expression being in the ovarian nurse cells and the central nervous system (CNS). The recent study of InR from the triatomine bug *Rhodnius prolixus* (5^{th} instar) demonstrated the highest expression of the InR gene in the CNS and in salivary glands (Defferrari et al., 2018). Two partial sequences almost identical to *Ir*InR (GenBank GBBN01007426 and GBBN01001068) could indeed be found in the synganglion transcriptome from the closely related species *I. scapularis* (Egekwu et al., 2014). We did not attempt to quantify the relative expression of *Ir*InR transcript in the synganglion of *I. ricinus* females given the difficulties associated with achieving a reliable dissection of this tissue. However, a relatively low expression of *Ir*InR transcript in the remaining parts of the tick body containing the synganglion (tagged as REST in Fig. 2A) does not indicate predominant levels of *Ir*InR mRNA in synganglions related to other tick tissues.

It is still an unresolved question whether the increasing expression of ISP components during feeding is caused by the initial digestion of nutrients or whether the increased expression of the ISP triggers activation of the tick digestive system (Sojka et al., 2013).

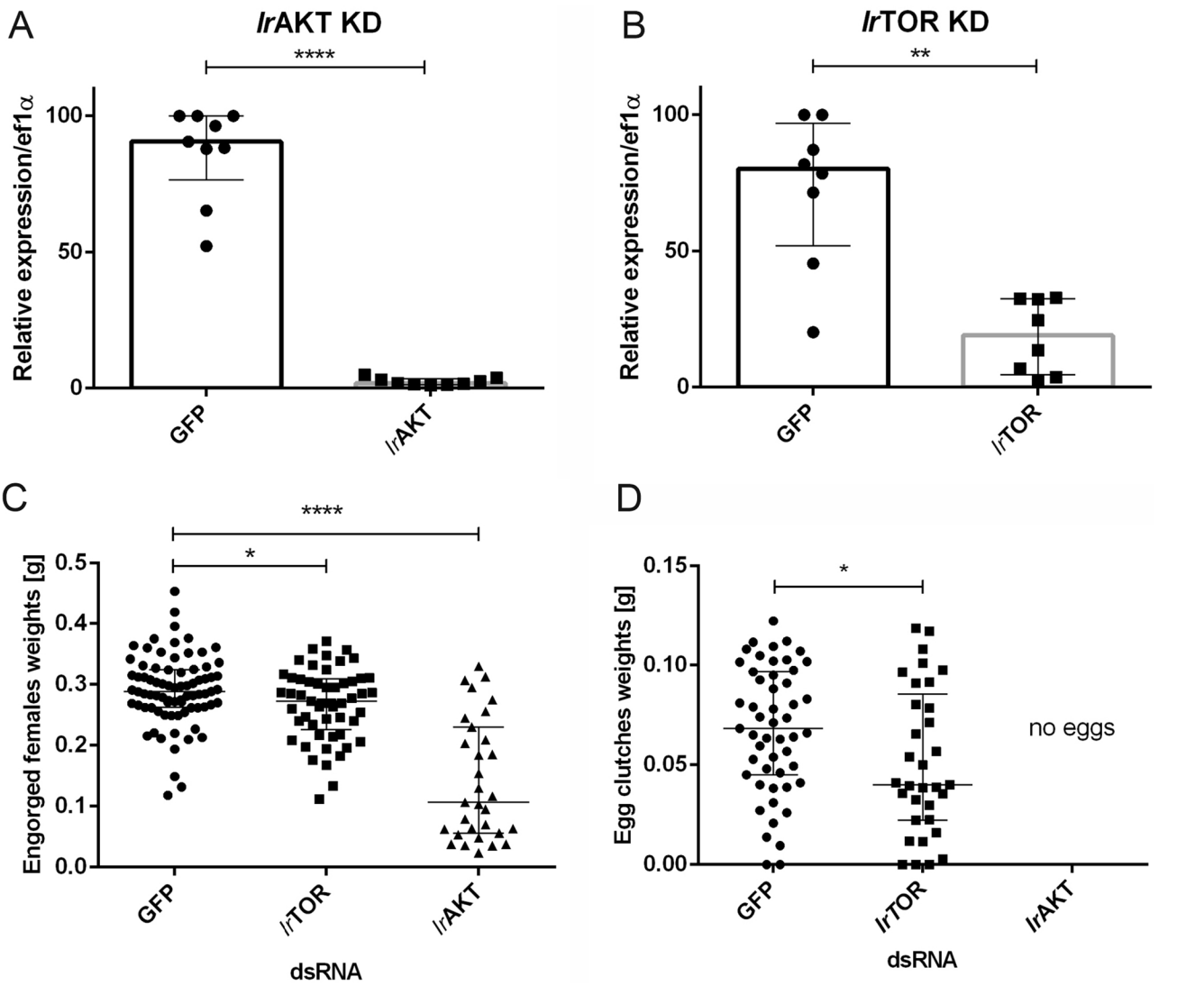

Fig. 4. RNAi knock down of *Ir*AKT, and *Ir*TOR and the effect on *Ixodes ricinus* phenotype.
(**A, B**) Verification of *Ir*AKT and *Ir*TOR RNAi knockdown efficiency from three independent experiments (three randomly selected females fed for 3 days were examined from each cohort). (**C**) The weight differences of *Ir*AKT and *Ir*TOR dsRNA injected females compared to the GFP control group. (**D**) The weights of eggs laid by *Ir*TOR dsRNA injected females compared to the GFP control group. No eggs were laid by females injected with *Ir*AKT dsRNA. Data were analyzed by the Mann-Whitney test: A—$P < 0.0001$; B—$P = 0.0019$; C—$P = 0.0433$ (GFP vs. *Ir*TOR) and $P < 0.0001$ (GFP vs. *Ir*AKT); D—$P = 0.0299$. Lines or columns indicate the medians; error bars indicate the interquartile rates.

The efficiency of RNAi KD of *Ir*InR was highly variable between individual females. However, feeding was clearly impaired in the females in which the *Ir*InR mRNA levels were markedly reduced upon injection of *Ir*InR dsRNA (Fig. 3D). In our experience, RNAi KD of membrane proteins is generally less effective and reproducible in comparison to the KD of secreted or intracellular proteins and the resulting phenotypes are often less expressed given the lower turnover rates of membrane proteins. A successful RNAi KD of the insulin receptor was reported in the tissues of the mosquito *Culex quinquefasciatus* (Nuss et al., 2018). Knock-down of the mosquito InR negatively affected trypsin-like activity in the midgut and ecdysteroid production in ovaries, and intriguingly, it blocked the larval development of the filarial parasite *Wuchereria bancrofti* in infected mosquitoes (Nuss et al., 2018). On the other hand, no clear phenotype was reported for InR KD in the kissing bug *R. prolixus* (Defferrari et al., 2018).

Despite the high similarity between human and tick insulin receptors, injection of mammalian insulin receptor antagonist S691 (Schaffer et al., 2008) into *I. ricinus* females did not impair tick feeding or oviposition (Supplementary Fig. S4). This result suggests that IRA is not capable of binding *Ir*InR with higher affinity than endogenous ILPs. Treatment of a mammalian breast cancer cell line with S691 down-regulated expression of InR and suppressed growth of the cancer cells (Sharma and Kumar, 2018), but injecting this compound into unfed *I. ricinus* females did not affect *Ir*InR expression in tick tissues (data not shown).

In contrast to the moderately reproducible effect of *Ir*InR KD, we observed much a stronger phenotype upon RNAi KD of the intracellular kinase *Ir*AKT. Ticks injected with *Ir*AKT dsRNA could not commence the rapid engorgement phase, even during prolonged feeding for about 2–3 d (Fig. 4C), and the partially fed females that dropped off the host produced no eggs (Fig. 4D). These results confirm the earlier RNAi-based functional study in the tick *H. longicornis,* demonstrating that *Hl*AKT is essential to complete the blood feeding process, accompanied by the growth of internal organs in adult ticks (Umemiya-Shirafuji et al., 2012b). Such a strong phenotype points to tick AKT as a potential drug target.

The function of TOR was previously examined in two tick species, *H. longicornis* (Umemiya-Shirafuji et al., 2012a) and, more recently, in

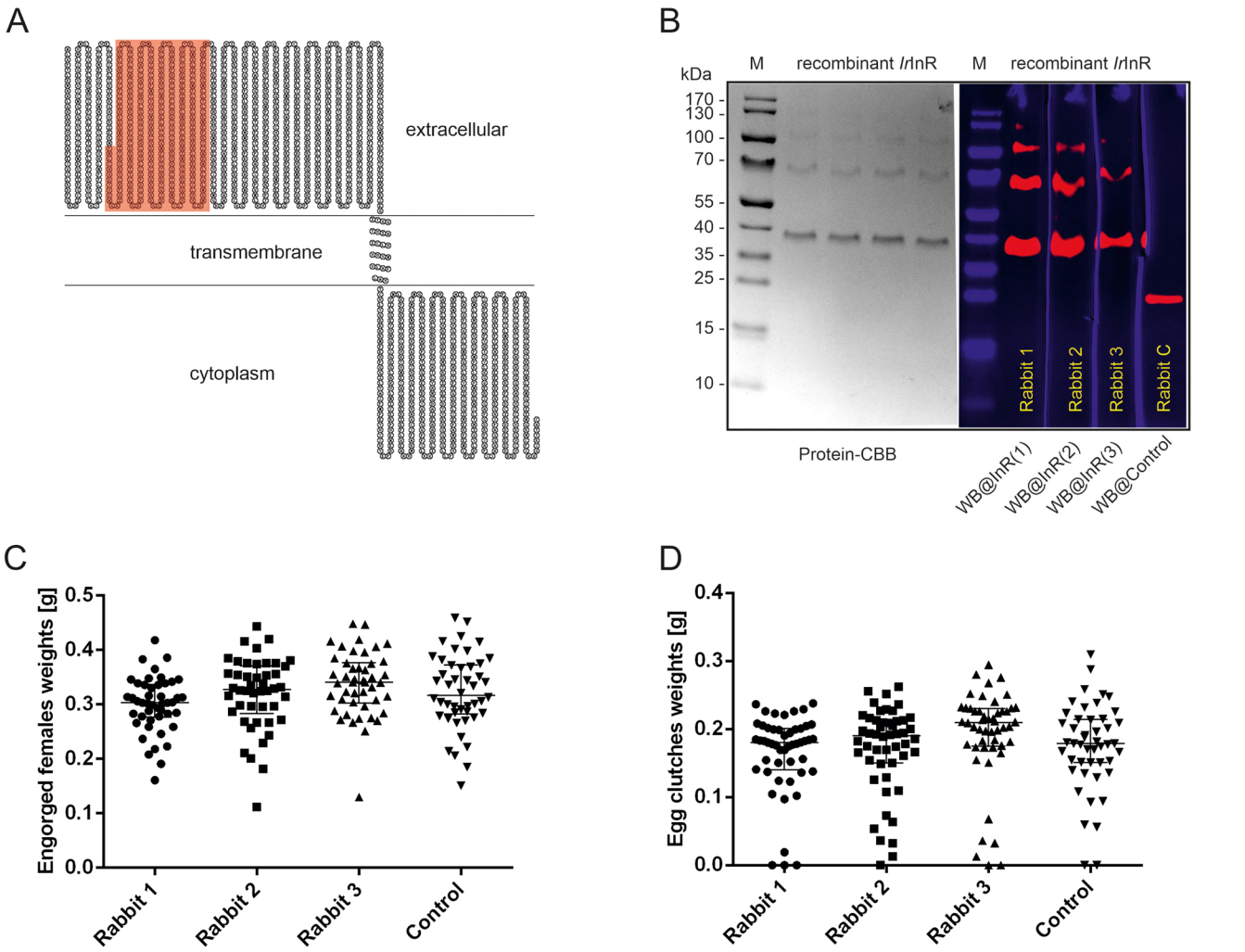

Fig. 5. Experimental vaccination of rabbits with a recombinant extracellular *Ir*InR fragment. (**A**) Distribution of extracellular, transmembrane and intracellular parts of *Ir*InR predicted using the TMHMM software (http://www.sacs.ucsf.edu/cgi-bin/tmhmm.py). Highlighted in red is the recombinant *Ir*InR fragment used for rabbit immunization (see also Supplementary Fig. S1). (**B**) Verification of the @*Ir*InR antibodies in the immunized rabbits. M – molecular markers; Protein-CBB – Protein load of the *Ir*InR recombinant fragment (200 ng of protein per lane) stained with Coomassie Brilliant Blue; WB@InR (1,2,3) and WB@Control – Western blotting with the sera of three immunized rabbits and one control rabbit, respectively. Primary antibody: Anti-*Ir*InR sera 1:5,000, secondary antibody: Anti-Rabbit/peroxidase conjugate 1:5,000. Visualized using ChemiDoc™ Imaging System (Bio-Rad). (**C**) Weights of fully engorged *Ixodes ricinus* females infested on immunized rabbits. Statistical analysis (Mann-Whitney test) did not show any significant differences between immunized and control rabbits. (**D**) Weights of eggs laid by the females infested on immunized rabbits. Statistical analysis (Mann-Whitney test) did not show any significant differences between immunized and control rabbits. Lines indicate the medians; error bars indicate the interquartile rates. (For interpretation of the references to colour in this figure legend, the reader is referred to the web version of this article).

R. microplus (Waltero et al., 2019). Both studies demonstrated that TOR gene silencing had little or no effect on tick feeding but strongly reduced the synthesis of yolk proteins (vitellogenins), production of eggs in ovaries, and heavily impaired embryonic development and larval hatching. Despite quite efficient reduction of *Ir*TOR mRNA levels upon injection of *Ir*TOR dsRNA (Fig. 4B), we observed only slightly reduced post-engorgement weights of *I. ricinus* females and egg production (Fig. 4C, D). The reason for this difference remains unclear.

To test the sensitivity of *Ir*AKT and *Ir*TOR to commercially available inhibitors, we administered specific AKT inhibitor A-443654 (Han et al., 2007) and TOR inhibitor rapamycin (Vezina et al., 1975) to *I. ricinus* females via *in vitro* membrane feeding (Perner et al., 2016b). However, the tested inhibitor concentrations ranging from 10 nM up to 100 μM did not cause any significant differences in weight distribution between females membrane-fed on the diet with the inhibitors and their solvents used as a mock (Supplementary Fig. S 5A, B).

Although RNAi KD is often presented as a useful tool for the discovery of candidate anti-tick protective antigens, reported cases demonstrating a strong RNAi-based phenotype confirmed by a subsequent successful experimental vaccination with a respective recombinant molecule are still quite rare (de la Fuente et al., 2016). Tick midgut membrane proteins, such as Bm86 from the cattle tick *R. microplus* (Willadsen et al., 1995), represent intuitively the first line targets that can be blocked by antibodies ingested in blood from immunized hosts (Richards et al., 2015). Despite our theoretical expectations on *Ir*InR, experimental vaccination with the extracellular domain of this molecule had no effect on tick feeding and reproduction (Fig. 5). This result suggests that *Ir*InR extracellular domain most likely does not face the midgut lumen to bind to the exogenous insulin of host origin but rather serves as receptor for endogenous ILPs at the midgut epithelium-hemocoel interface. This explanation is further supported by the recent identification of four insulin-like peptides (*Is*ILP1, *Is*ILP3, *Is*ILP4, and *Is*ILP5) in *I. scapularis* (Sharma et al., 2019a) that most likely act as the natural ligands of tick InR. The tissue expression profiles of *Is*ILPs show some tissue specificity, e.g. *Is*ILP1 and 5 were reported mainly to be expressed in the synganglion, while *Is*ILP3 and 4 are more

specific for salivary glands. In contrast to the expression of *Ir*InR shown here, the authors reported the highest expression of most *Is*ILPs in unfed ticks and very low expression in *I. scapularis* ovaries (Sharma et al., 2019a). We could find clear orthologs of *I. scapularis* ILPs tagged accordingly as *Ir*ILP1, *Ir*ILP3, *Ir*ILP4 in the *I. ricinus* midgut and salivary gland transcriptomes (GenBank: GANP01002380, GANP01014446, GANP01013821, respectively) (Kotsyfakis et al., 2015a), and *Ir*ILP5 in the *I. ricinus* whole body transcriptome (GenBank: GIDG01004499) (Vechtova et al., 2020). The existence of several ILPs and only one form of InR suggests that the specificity of the endocrine regulation controlled by ISP in different tick organs is determined by the expressional dynamics and spatial distribution of tick ILPs. The elegant study demonstrating the specific role of *Aedes aegypti* ILP3 in mosquito metabolism and egg maturation (Brown et al., 2008), and other studies on the function of ILPs in mosquitoes (reviewed by (Sharma et al., 2019b) encouraged us to focus next on a functional study of individual tick ILPs and to decipher their specific roles in physiological processes controlled by tick ISP.

Altogether, the molecular and functional characterization of insulin receptor from *I. ricinus* adds an important piece of knowledge on ISP in ticks. Our tissue expression data as well as RNAi KD of *Ir*InR and the downstream intracellular kinases *Ir*AKT *and Ir*TOR imply that tick ISP is involved in tick feeding, development, and reproduction. Investigating the specific physiological roles that tick ISP plays in the nutritional status sensing, regulation of the digestive system, vitellogenesis, and embryogenesis presents exciting challenges for future studies.

CRediT authorship contribution statement

Tereza Kozelková: Investigation, Data curation, Writing - original draft. **David Doležel:** Investigation, Data curation. **Lenka Grunclová:** Investigation, Methodology. **Matěj Kučera:** Methodology. **Jan Perner:** Data curation, Supervision, Validation. **Petr Kopáček:** Conceptualization, Project administration, Supervision, Funding acquisition, Writing - review & editing.

Declaration of Competing Interest

The authors report no declarations of interest.

Acknowledgements

This project was primarily supported by the Czech Science Foundation (GAČR) No. 18-01832S to P.K. and by the project OPVVV CZ.02.1.01/0.0/0.0/16_019/0000759 funded by the European Structural and Investment Funds (ESIF) and Ministry of Education, Youth and Sport (MEYS) to P.K., J.P., and M.K. The authors gratefully acknowledge the technical assistance of Jan Erhart from the tick rearing facility at the Institute of Parasitology, BC CAS (RVO 60077344).

Appendix A. Supplementary data

Supplementary material related to this article can be found, in the online version, at doi:https://doi.org/10.1016/j.ttbdis.2021.101694.

References

Ahlers, L.R.H., Trammell, C.E., Carrell, G.F., Mackinnon, S., Torrevillas, B.K., Chow, C.Y., Luckhart, S., Goodman, A.G., 2019. Insulin potentiates JAK/STAT signaling to broadly inhibit flavivirus replication in insect vectors. Cell Rep. 29, 1946–1960.

Badisco, L., Van Wielendaele, P., Vanden Broeck, J., 2013. Eat to reproduce: a key role for the insulin signaling pathway in adult insects. Front. Physiol. 4, 202.

Brown, M.R., Clark, K.D., Gulia, M., Zhao, Z., Garczynski, S.F., Crim, J.W., Suderman, R. J., Strand, M.R., 2008. An insulin-like peptide regulates egg maturation and metabolism in the mosquito *Aedes aegypti*. Proc. Natl. Acad. Sci. U. S. A. 105, 5716–5721.

Davis, H.H., Dotson, E.M., Oliver Jr, J.H., 1994. Localization of insulin-like immunoreactivity in the synganglion of nymphal and adult *Dermacentor variabilis* (Acari: Ixodidae). Exp. Appl. Acarol. 18, 111–122.

de Abreu, L.A., Fabres, A., Esteves, E., Masuda, A., da Silva Vaz Jr, I., Daffre, S., Logullo, C., 2009. Exogenous insulin stimulates glycogen accumulation in *Rhipicephalus* (*Boophilus*) *microplus* embryo cell line BME26 via PI3K/AKT pathway. Comp. Biochem. Physiol. B Biochem. Mol. Biol. 153, 185–190.

de la Fuente, J., Estrada-Pena, A., Venzal, J.M., Kocan, K.M., Sonenshine, D.E., 2008. Overview: ticks as vectors of pathogens that cause disease in humans and animals. Front. Biosci. 13, 6938–6946.

de la Fuente, J., Kopacek, P., Lew-Tabor, A., Maritz-Olivier, C., 2016. Strategies for new and improved vaccines against ticks and tick-borne diseases. Parasite Immunol. 38, 754–769.

De Meyts, P., Whittaker, J., 2002. Structural biology of insulin and IGF1 receptors: implications for drug design. Nat. Rev. Drug Discov. 1, 769–783.

Defferrari, M.S., Da Silva, S.R., Orchard, I., Lange, A.B., 2018. A *Rhodnius prolixus* insulin receptor and its conserved intracellular signaling pathway and regulation of metabolism. Front. Endocrinol (Lausanne) 9, 745.

Donohue, K.V., Khalil, S.M., Ross, E., Grozinger, C.M., Sonenshine, D.E., Michael Roe, R., 2010. Neuropeptide signaling sequences identified by pyrosequencing of the American dog tick synganglion transcriptome during blood feeding and reproduction. Insect Biochem. Mol. Biol. 40, 79–90.

Dupont, J., LeRoith, D., 2001. Insulin and insulin-like growth factor I receptors: similarities and differences in signal transduction. Horm. Res. 55, 22–26.

Egekwu, N., Sonenshine, D.E., Bissinger, B.W., Roe, R.M., 2014. Transcriptome of the female synganglion of the black-legged tick *Ixodes scapularis* (Acari: Ixodidae) with comparison between Illumina and 454 systems. PLoS One 9 e102667.

Hajdusek, O., Sojka, D., Kopacek, P., Buresova, V., Franta, Z., Sauman, I., Winzerling, J., Grubhoffer, L., 2009. Knockdown of proteins involved in iron metabolism limits tick reproduction and development. Proc. Natl. Acad. Sci. U. S. A. 106, 1033–1038.

Hajdusek, O., Almazan, C., Loosova, G., Villar, M., Canales, M., Grubhoffer, L., Kopacek, P., de la Fuente, J., 2010. Characterization of ferritin 2 for the control of tick infestations. Vaccine 28, 2993–2998.

Han, E.K., Leverson, J.D., McGonigal, T., Shah, O.J., Woods, K.W., Hunter, T., Giranda, V.L., Luo, Y., 2007. Akt inhibitor A-443654 induces rapid Akt Ser-473 phosphorylation independent of mTORC1 inhibition. Oncogene 26, 5655–5661.

Hernandez-Sanchez, C., Mansilla, A., de Pablo, F., Zardoya, R., 2008. Evolution of the insulin receptor family and receptor isoform expression in vertebrates. Mol. Biol. Evol. 25, 1043–1053.

Kaufman, W.R., 2007. Gluttony and sex in female ixodid ticks: how do they compare to other blood-sucking arthropods? J. Insect Physiol. 53, 264–273.

Kotsyfakis, M., Schwarz, A., Erhart, J., Ribeiro, J.M., 2015a. Tissue- and time-dependent transcription in *Ixodes ricinus* salivary glands and midguts when blood feeding on the vertebrate host. Sci. Rep. 5, 9103.

Kotsyfakis, M., Kopacek, P., Franta, Z., Pedra, J.H.F., Ribeiro, J.M.C., 2015b. Deep sequencing analysis of the *Ixodes ricinus* haemocytome. PLoS Negl. Trop. Dis. 9 e0003754.

Kremer, L.P.M., Korb, J., Bornberg-Bauer, E., 2018. Reconstructed evolution of insulin receptors in insects reveals duplications in early insects and cockroaches. J. Exp. Zool. B Mol. Dev. Evol. 330, 305–311.

Lin, X., Xu, Y., Jiang, J., Lavine, M., Lavine, L.C., 2018. Host quality induces phenotypic plasticity in a wing polyphenic insect. Proc. Natl. Acad. Sci. U. S. A. 115, 7563–7568.

Luckhart, S., Riehle, M.A., 2007. The insulin signaling cascade from nematodes to mammals: insights into innate immunity of *Anopheles* mosquitoes to malaria parasite infection. Dev. Comp. Immunol. 31, 647–656.

Mans, B.J., de Castro, M.H., Pienaar, R., de Klerk, D., Gaven, P., Genu, S., Latif, A.A., 2016. Ancestral reconstruction of tick lineages. Ticks Tick Borne Dis. 7, 509–535.

Nagasawa, H., Kataoka, H., Isogai, A., Tamura, S., Suzuki, A., Ishizaki, H., Mizoguchi, A., Fujiwara, Y., Suzuki, A., 1984. Amino-terminal amino acid sequence of the silkworm prothoracicotropic hormone: homology with insulin. Science 226, 1344–1345.

Nijhof, A.M., Balk, J.A., Postigo, M., Jongejan, F., 2009. Selection of reference genes for quantitative RT-PCR studies in *Rhipicephalus* (*Boophilus*) *microplus* and *Rhipicephalus appendiculatus* ticks and determination of the expression profile of Bm86. BMC Mol. Biol. 10, 112.

Nuss, A.B., Brown, M.R., Murty, U.S., Gulia-Nuss, M., 2018. Insulin receptor knockdown blocks filarial parasite development and alters egg production in the southern house mosquito, *Culex quinquefasciatus*. PLoS Negl. Trop. Dis. 12 e0006413.

Perner, J., Provaznik, J., Schrenkova, J., Urbanova, V., Ribeiro, J.M., Kopacek, P., 2016a. RNA-seq analyses of the midgut from blood- and serum-fed *Ixodes ricinus* ticks. Sci. Rep. 6, 36695.

Perner, J., Sobotka, R., Sima, R., Konvickova, J., Sojka, D., Oliveira, P.L., Hajdusek, O., Kopacek, P., 2016b. Acquisition of exogenous haem is essential for tick reproduction. Elife 5 e12318.

Perner, J., Kropackova, S., Kopacek, P., Ribeiro, J.M.C., 2018. Sialome diversity of ticks revealed by RNAseq of single tick salivary glands. PLoS Negl. Trop. Dis. 12 e0006410.

Pfaffl, M.W., 2001. A new mathematical model for relative quantification in real-time RT-PCR. Nucleic Acids Res. 29, e45.

Richards, S.A., Stutzer, C., Bosman, A.M., Maritz-Olivier, C., 2015. Transmembrane proteins–Mining the cattle tick transcriptome. Ticks Tick Borne Dis. 6, 695–710.

Schaffer, L., Brand, C.L., Hansen, B.F., Ribel, U., Shaw, A.C., Slaaby, R., Sturis, J., 2008. A novel high-affinity peptide antagonist to the insulin receptor. Biochem. Biophys. Res. Commun. 376, 380–383.

Sharma, P., Kumar, S., 2018. S961, a biosynthetic insulin receptor antagonist, downregulates insulin receptor expression & suppresses the growth of breast cancer cells. Indian J. Med. Res. 147, 545–551.

Sharma, A., Pooraiiouby, R., Guzman, B., Vu, P., Gulia-Nuss, M., Nuss, A.B., 2019a. Dynamics of insulin signaling in the black-legged tick, *Ixodes scapularis*. Front. Endocrinol. (Lausanne) 10, 292.

Sharma, A., Nuss, A.B., Gulia-Nuss, M., 2019b. Insulin-like peptide signaling in mosquitoes: the road behind and the road ahead. Front. Endocrinol. (Lausanne) 10, 166.

Smykal, V., Pivarci, M., Provaznik, J., Bazalova, O., Jedlicka, P., Luksan, O., Horak, A., Vaneckova, H., Benes, V., Fiala, I., Hanus, R., Dolezel, D., 2020. Complex evolution of insect insulin receptors and homologous decoy receptors, and functional significance of their multiplicity. Mol. Biol. Evol. 37, 1775–1789.

Sojka, D., Franta, Z., Horn, M., Caffrey, C.R., Mares, M., Kopacek, P., 2013. New insights into the machinery of blood digestion by ticks. Trends Parasitol. 29, 276–285.

Sonenshine, D.E., Roe, R.M., 2014. Biology of Ticks, 2 ed. Oxford University Press.

Trifinopoulos, J., Nguyen, L.T., von Haeseler, A., Minh, B.Q., 2016. W-IQ-TREE: a fast online phylogenetic tool for maximum likelihood analysis. Nucleic Acids Res. 44, W232–235.

Umemiya-Shirafuji, R., Boldbaatar, D., Liao, M., Battur, B., Rahman, M.M., Kuboki, T., Galay, R.L., Tanaka, T., Fujisaki, K., 2012a. Target of rapamycin (TOR) controls vitellogenesis via activation of the S6 kinase in the fat body of the tick, *Haemaphysalis longicornis*. Int. J. Parasitol. 42, 991–998.

Umemiya-Shirafuji, R., Tanaka, T., Boldbaatar, D., Tanaka, T., Fujisaki, K., 2012b. Akt is an essential player in regulating cell/organ growth at the adult stage in the hard tick *Haemaphysalis longicornis*. Insect Biochem. Mol. Biol. 42, 164–173.

Vafopoulou, X., 2014. The coming of age of insulin-signaling in insects. Front. Physiol. 5, 216.

Vechtova, P., Fussy, Z., Cegan, R., Sterba, J., Erhart, J., Benes, V., Grubhoffer, L., 2020. Catalogue of stage-specific transcripts in *Ixodes ricinus* and their potential functions during the tick life-cycle. Parasit. Vectors 13, 311.

Vezina, C., Kudelski, A., Sehgal, S.N., 1975. Rapamycin (AY-22,989), a new antifungal antibiotic. I. Taxonomy of the producing streptomycete and isolation of the active principle. J. Antibiot. (Tokyo) 28, 721–726.

Waltero, C., de Abreu, L.A., Alonso, T., Nunes-da-Fonseca, R., da Silva Vaz Jr, I., Logullo, C., 2019. TOR as a regulatory target in *Rhipicephalus microplus* embryogenesis. Front. Physiol. 10, 965.

Willadsen, P., Bird, P., Cobon, G.S., Hungerford, J., 1995. Commercialisation of a recombinant vaccine against *Boophilus microplus*. Parasitology 110 (Suppl), S43–50.

Wu, Q., Brown, M.R., 2006. Signaling and function of insulin-like peptides in insects. Annu. Rev. Entomol. 51, 1–24.

Xu, H.J., Xue, J., Lu, B., Zhang, X.C., Zhuo, J.C., He, S.F., Ma, X.F., Jiang, Y.Q., Fan, H. W., Xu, J.Y., Ye, Y.X., Pan, P.L., Li, Q., Bao, Y.Y., Nijhout, H.F., Zhang, C.X., 2015. Two insulin receptors determine alternative wing morphs in planthoppers. Nature 519, 464–467.

Zhu, X.X., Oliver Jr, J.H., 1991. Immunocytochemical localization of an insulin-like substance in the synganglion of the tick *Ornithodoros parkeri* (Acari: Argasidae). Exp. Appl. Acarol. 13, 153–159.